USP22 overexpression fails to augment tumor formation in MMTV-ERBB2 mice but loss of function impacts MMTV promoter activity

Xianghong Kuang[1,2], Andrew Salinger[1, 2], Fernando Benavides[1, 2], William J. Muller[3, 4, 5], Sharon Y. R. Dent[1, 2, 6 *] and Evangelia Koutelou[1, 2 *]

[1]Department of Epigenetics and Molecular Carcinogenesis, The University of Texas MD Anderson Cancer Center, Houston, TX 77054, USA

[2] Center for Cancer Epigenetics, The University of Texas MD Anderson Cancer Center, Houston, TX 77030, USA

[3] Rosalind and Morris Goodman Cancer Institute, McGill University, Montreal, Canada.

[4] Department of Biochemistry, McGill University, Montreal, Canada.

[5] Faculty of Medicine, McGill University, Montreal, Canada.

[6] The University of Texas MD Anderson Cancer Center/UTHealth Houston Graduate School of Biomedical Sciences

[*]**Corresponding authors:** Sharon Y. R. Dent and Evangelia Koutelou, Department of Epigenetics and Molecular Carcinogenesis, The University of Texas MD Anderson Cancer Center, PO Box 301429, Unit 1951 Houston, Texas 77230, USA. Phone number: 713-563-7742. Email: sroth@mdanderson.org (S.Y.R.D.); ekoutelou@mdanderson.org (E.K.)

Running title: Usp22 impacts on MMTV-NIC tumorigenesis

Key Words: Usp22, MMTV, Mammary gland tumorigenesis, ERBB2, Neu

Funding resource: The National Institutes of Health grant R01HD094400 to S.Y.R. Dent.

Abstract

The USP22 deubiquitinase, a component of the SAGA histone modifying complex, is overexpressed in multiple human cancers, but how USP22 impacts tumorigenesis is not clear. We reported previously that *Usp22* loss in mice impacts execution of several signaling pathways driven by growth factor receptors such as ERBB2. To determine whether changes in USP22 expression affects ERBB2-driven tumorigenesis, we introduced conditional overexpression or deletion alleles of *Usp22* into mice bearing the MMTV-NIC transgene, which drives both rat ERBB2/NEU expression and Cre recombinase activity from the MMTV promoter resulting in mammary tumor formation. We found that USP22 overexpression in mammary glands did not further enhance primary tumorigenesis in MMTV-NIC female mice, but increased lung metastases were observed. However, deletion of *Usp22* significantly decreased tumor burden and increased survival of MMTV-NIC mice. These effects were associated with markedly decreased levels of both *Erbb2* mRNA and protein, indicating *Usp22* loss impacts MMTV promoter activity. *Usp22* loss had no impact on ERBB2 expression in other settings, including MCF10A cells bearing a CMV-driven *ERBB2* transgene or in HER2+ human SKBR3 and HCC1953 cells. Decreased activity of the MMTV promoter in MMTV-NIC mice correlated with decreased expression of known regulatory factors, including the glucocorticoid receptor (GR), the progesterone receptor (PR), and the chromatin remodeling factor BRG1. Together our findings indicate that increased expression of USP22 does not augment the activity of an activated ERBB2/NEU transgene, but impacts of Usp22 loss on tumorigenesis cannot be assessed in this model due to unexpected effects on MMTV-driven Erbb2/Neu expression.

Significance

Overexpression of USP22 alone is not sufficient to promote MMTV-ERBB2-driven tumor formation but may enhance metastasis. *Usp22* loss impacts expression of GR, PR and BRG1, decreasing MMTV promoter activity.

Introduction

USP22 overexpression occurs in several types of highly aggressive human cancers and is associated with a “death from cancer” gene signature for therapy resistance and stem cell like phenotypes (1-3). How USP22 impacts cancer development and progression, however, is still not well defined.

USP22 provides the catalytic activity of the deubiquitinase (DUB) module of the SAGA histone modifying complex. SAGA complex is multifunctional, housing both DUB and histone lysine acetyltransferase (KAT) activities, along with factors that interact directly with either sequence specific or general transcription factors to activate genes. Both the KAT and DUB modules of SAGA have been implicated in human cancers (1). The catalytic subunit of the KAT module, GCN5/KAT2A, is an important co-activator of MYC target genes during normal mouse development and in human cancer cells (4-6). Deletion or inhibition of *Gcn5* impacts growth and survival of MYC-driven cancers, including lung cancers and lymphoma, in both mouse models and human cells (5,7). USP22 functions have also been linked to MYC and other oncogenes, including BMI1, SIRT1, cyclin B1 and KDM1A (8-11). These findings support a role for USP22 and SAGA in promoting cell proliferation. USP22 impact on proliferation is further indicated by connections between USP22, the androgen receptor and c-MYC in prostate cancer cells and models (12). Other studies, however, indicate that USP22 also functions to suppress tumor formation in particular contexts, such as colorectal cancer (13). In all cases, the functions of USP22 in cancer may reflect its activity towards histone substrates and gene regulation or to removal of ubiquitin from non-histone substrates by USP22 that may impact other processes, such as telomere stability or DNA repair (14,15).

In order to better define USP22 functions in cancer, we created mouse models to determine its functions during normal development. Deletion of *Usp22* leads to embryonic lethality due to defects in placental vasculature (16). Gene expression changes indicate that these defects are linked to aberrant execution of multiple receptor tyrosine kinase signaling cascades as well as TGFβ signaling that drive propagation of endothelial cells, specification of perivascular cells, and cell migration (16). These same pathways and processes are often associated with tumorigenesis, so we also created a Lox-Stop-Lox mouse model that overexpresses USP22 in all tissues to determine whether overexpression is sufficient for induction of these pathways. We observed over branching of the mammary glands in USP22 overexpressing mice, along with

aberrant up regulation of many of the same signaling pathways that were down regulated in *Usp22* null embryos, including estrogen receptor, ERK/MAPK, and TGFβ signaling (16,17). However, USP22 overexpression was not sufficient to induce tumors in the mammary gland or in any other tissues (17), suggesting this DUB likely works with specific oncogenes to promote tumorigenesis.

ERBB2 was one of the signaling pathways impacted by *Usp22* loss (16). Overexpression of ERBB2 (also known as HER2/NEU) is associated with human breast cancers, and mouse models of HER2+ tumors, including MMTV-NIC transgenic mice (expressing an activated oncogenic human *ERBB2*), have provided many insights into how ERBB2 induces tumors and promotes metastases (18-20). One previous study by others indicated that USP22 regulates the unfolded protein response in HER2+ tumors (21). Here we combine the MMTV-NIC transgene with either USP22 overexpression or *Usp22* loss to determine whether and how this DUB impacts ERBB2 driven oncogenesis in mice.

Materials and Methods

Mouse models

To generate bigenic mice that specifically overexpress Usp22 in mouse mammary gland epithelium (*Usp22*$^{OE/OE}$; MMTV-NIC**)**, we crossed our lab generated *Rosa26KI-Usp22-LSL* mice (congenic FVB/N background) (17) with MMTV-NIC (MMTV-Neu (NDL2-5)-IRES-Cre, JAX Strain # 032576) mice on pure FVB/N background (generous gift from Dr. William J. Muller) (22). We identified mice bearing desired genotypes by PCR, using allele-specific primers, 5' AAAGTCCCTATTGGCGTTACTA 3' (forward) and 5' AAAGTCGCTCTGAGTTGTTATC 3' (reverse) for the knock-in allele with a product size of 388 bp. PCR primers for the wild-type Rosa26 locus had the sequences 5' GGAGCGGGAGAAATGGATAT 3' (forward) and 5' AAAGTCGCTCTGAGTTGTTATC 3' (reverse), producing a PCR product size of 602 bp. The PCR program ran 35 cycles of 95ºC, 5 min, for denaturing; 55ºC, 40 sec, for annealing; and 72ºC, 1 min, for extension.

To generate mice bearing a *Usp22* floxed allele, we obtained sperm bearing the *Usp22*$^{tm1a(KOMP)Wtsi}$ allele (C57BL/6N) from the Wellcome Trust KOMP consortium (www.komp.org) and performed *in vitro* fertilization. The *Usp22*$^{tm1a(KOMP)Wtsi}$ allele contains two LoxP sites surrounding exon 2 of *Usp22* and a neomycin selection cassette surrounded by two short flippase recognition target

135 (FRT) sites. We crossed mice bearing the *Usp22*$^{tm1a(KOMP)Wtsi}$ allele with FLPeR mice (obtained
136 from the Genetically Engineered Mouse Facility, MD Anderson Cancer Center) expressing a
137 flippase expression construct (23), in order to remove the neomycin cassette. The resulting
138 Usp22$^{FL/+}$ or Usp22$^{FL/FL}$ mice were backcrossed several times onto FVB/NHsd (Envigo,
139 Indianapolis, IN) using marker-assisted (speed congenics) crosses (Laboratory Animal Genetic
140 Services, MD Anderson Cancer Center), and then crossed with MMTV-NIC mice (also in the
141 FVB/N background) to achieve mammary gland epithelial-specific *Usp22* deletion. Genotypes
142 were determined by PCR using primers CSD-*Usp22*-F (forward): 5'
143 ACTTTGGGAAAGCTCGTATGTGTGC 3' and CSD-*Usp22*-ttR (reverse): 5'
144 GATGACATCATCACATTCCCACGCC 3' yielding a PCR product of 486bp for the wildtype allele
145 and 623bp for the floxed allele.
146
147 **Detection of mammary gland tumors**
148
149 Mouse mammary gland tumor onset in female mice was monitored by palpation twice weekly
150 starting from 10-weeks of age. Tumor size was measured by caliber and mice were sacrificed
151 when the largest tumor diameter reached 2 cm. Tumor volume was estimated with the formula:
152 volume = $(\text{width})^2$ X length/2 (cm^3). All animal experiments were conducted under the guidelines
153 of the Institutional Animal Care and Use Committee of UT MD Anderson Cancer Center and
154 approved animal protocols.

155 **Isolation of primary mouse mammary gland epithelial cells (MECs)**

156 The left and right 2nd, 3rd, and 4th mammary glands were dissected from 100-day-old female
157 *Usp22*$^{FL/FL}$-NIC and wildtype-NIC mice, with lymph nodes removed from the 4th glands. Organoids
158 were prepared from the dissected tissue as described (17,24) with modifications. Briefly, glands
159 were minced into paste and incubated in 5 mL DME/F-12 medium (HyClone, #SH30023.1) with
160 2 mg/mL collagenase A (Roche #10103578001), 100 units/mL hyaluronidase (Sigma-Aldrich,
161 H3506) for 1 h at 37°C with 180 rpm rotation. The resulting cell mixture was collected by
162 centrifugation and then washed with DME/F-12 medium and centrifuged twice at 450 g for 10 min
163 to remove the fatty layer. The cells were next incubated in 3 mL DME/F-12 medium with 2 units/mL
164 DNase I (Sigma-Aldrich, D4263) at room temperature for 3 min and centrifuged at 450 g for 10
165 min. The cell pellets were resuspended in 4 ml Red Blood Cell Lysis buffer (Ammonium Chloride
166 solution, Stemcell Technology, #07800) on ice for 2 min and washed with 6 mL DME/F-12 medium
167 at 450 g for 10 min. Differential centrifugation (pulse centrifugation to 450 g for 10 seconds) was

168 used to separate stroma from organoids. The supernatant from the second spin containing
169 fibroblasts, macrophages, and endothelial cells were discarded. The pellets from 2nd round pulse
170 centrifugations were organoids consisting mainly of mammary gland epithelial cells. The
171 organoids were then digested with 3 mL 0.05% Trypsin/EDTA (HyClone, #SH30236.1) with 2
172 unit/mL of DNase I for 3 min. An equal volume of DME/F-12 containing 10% fetal bovine serum
173 (FBS, Gibco, #10437-028) was added and the cells were dissociated by pipetting 20 times with a
174 1000 µL (size) tip. Isolated epithelial cells were then collected by 3 min centrifugation at 600g.

175

176 **Cell lines and cell culture**

177

178 MCF10A cells bearing either a vector control or an *ERBB2* overexpression construct (OE) were
179 generously provided by Dr. Dihua Yu (25). Cells were cultured in DME/F12 media supplemented
180 with 5% horse serum (Thermo Fisher Scientific, 16050122), 20 ng/mL hEGF (Sigma, E9644), 100
181 ng/mL cholera toxin (Sigma, C8052), 0.5 µg/mL hydrocortisone (Sigma, H0888), 10 µg/mL insulin
182 (Sigma, I1882), 50 units/mL penicillin, and 50 µg/mL streptomycin (Hyclone, #SV30010). DMEM
183 media (Hyclone #SH3002201) with 10% FBS was used to culture SKBR3 (the American Type
184 Culture Collection (ATCC), #HTB-30) and HCC1954 cells (ATCC, #CRL-2338).

185

186 **shRNA knockdown *USP22* in SKBR3, HCC1954 and MCF10A-*ERBB2* OE cells**

187

188 HEK293T cells at 70% confluency were co-transfected with lentiviral vectors expressing human
189 *USP22* shRNA. Vectors used included *pGIPZ-GFP-Puro* (see Supplementary Materials) and
190 *psPAX.2* and *pMD2.G* (Addgene). Cell transfections were done in Opti-MEM (Life Technologies,
191 #31985-070) using Lipofectamine 2000 (Life Technologies, Cat. # 11668019) following the
192 manufacturers' transfection reagent manual. Eight hours after the transfection, the medium was
193 changed to DMEM complete medium (DMEM medium with 10% FBS), and 48 hours post
194 transfection, the DMEM medium containing viral particles was collected and filtered through 0.45
195 µm filters. The virus containing medium with 8 µg/mL polybrene (Sigma-Aldrich, Cat #H9268) was
196 used in 1:1 dilution with the culture medium to infect SKBR3 and HCC1954 cells. 48 hours after
197 infection, the viral medium was changed to DMEM complete medium containing puromycin (EMD
198 Millipore, #540222) at 2 µg/mL for selection of infected cells. Since MCF10A-*ERBB2* cells are
199 already puromycin resistant, transfected cells were sorted on a BD FACSAria Fusion flow
200 cytometer (BD Biosciences) using a 100 µm tip at 70 psi to select for GFP+ cells (comparing

201 transfected cells to un-transfected cells) and were stained with Propidium Iodide to monitor
202 viability. Selected GFP+ cells were collected in a 15mL conical tube with 2mL FBS and then
203 expanded by cell culture in MCF10A culture medium.
204

205 **CRISPR-Cas9 *USP22* knock out in MCF10A-ERBB2 cells**

206 USP22 was deleted in MCF10A-*ERBB2* OE cells using Synthego Gene Knock out Kit v2,
207 Transfection Optimization Kit and Lipofectamine CRISPRMAX Transfection Reagent (Invitrogen,
208 #CMAX00003) according to Synthego's instructions (www.synthego.com/resources). Briefly, 70%
209 confluent MCF10A-*ERBB2* OE cells were trypsinized, washed and resuspended in OPTI-MEM
210 media. Ribonucleoprotein (RNP) complexes that consist of purified Cas9 nuclease duplexed with
211 chemically modified synthetic multi-guide sgRNA (sgRNA Usp22 KO, from Synthego's Gene
212 Knockout Kit v2) at a ratio of 1:1.3, or a non-sgRNA control in Opti-MEM media were then mixed
213 with lipofectamine CRISPRMAX transfection reagent at a volume ratio of 50:3. The RNP-
214 transfection solution mixture was then mixed with MCF10A-*ERBB2* OE cell suspensions and
215 seeded on cell culture plates. *USP22* knock out cells and non-sgRNA control cells were collected
216 and knock out efficiencies were validated by immunoblot analyses.

217 **Immunoblotting**

218 Isolated MECs, pelleted cells or tumor samples were lysed in RIPA buffer (150 mM NaCl, 0.1%
219 SDS, 50mM Tris (pH 7.4), 0.5% deoxycholic acid, 1% Nonidet P-40) with protease inhibitor
220 cocktail (Sigma, #P8340) and phosphatase inhibitors PhosSTOP (Roche, #04906837001). The
221 extracts were mixed with Laemmli buffer and boiled at 95°C for 5 min. The lysates (20 - 30 µg of
222 total protein) were subjected to electrophoresis on NuPAGE 4-12% Bis-Tris gels (Invitrogen,
223 NP0322BOX), transferred to PVDF membranes (BIO-RAD, #1620177), and probed with primary
224 and secondary antibodies. Antibody information is available in Supplementary Materials. ECL
225 reagents were from Amersham (#RPN2236).

226 **RNA isolation and qRT-PCR**

227 Total RNA from mouse tissues, cell lines or mammary gland epithelial cells were extracted using
228 RNeasy Plus Mini Kit (Qiagen, #74136). Extracts were then treated with RNase free DNase
229 (Qiagen, #79254). qRT-PCR products were measured using Power SYBR Green RNA-to-Ct 1-
230 step kit (Applied Biosystem, #4389986) and the 7500 Fast Real-Time PCR System (Applied

231 Biosystems). Sequences for gene-specific qRT-PCR primers used are listed in the
232 Supplementary Materials. Expression of *GAPDH* (human) or *Pbgd* (mouse) was used as internal
233 control. Data were normalized by the expression levels of internal control and the relative
234 expression of RNAs was calculated using the comparative Ct method.

235 **Statistical analysis**

236

237 All data were represented as mean ±standard error of mean. Calculations for qRT-PCR were
238 performed in Microsoft Excel. The Log-rank (Mantel–Cox) test was used as statistical analysis for
239 Kaplan-Meier tumor-free survival curves. All other statistical analysis was performed in Prism
240 9 (GraphPad Prism Software 9.0) using two-tailed unpaired t test. * p value <0.05, ** p< 0.01 and
241 ***p<0.001.

242

243 **Results**

244

245 **USP22 Overexpression in MMTV-NIC mice**

246

247 To determine whether Usp22 overexpression might enhance ERBB2-driven formation of
248 mammary tumors, we introduced our previously described *Lox-Stop-Lox (LSL) Usp22* allele (17)
249 into mice carrying the MMTV-NIC transgene (**Fig. 1A**). The *LSL Usp22* allele inserted at the
250 *Rosa26* locus allows tissue-specific overexpression (OE) of USP22 upon exposure to Cre
251 recombinase (17). The USP22 protein expressed from the *OE/LSL* allele (hereafter referred to
252 as *OE*) is fully functional and can fully rescue lethality of *Usp22* null embryos, but it is not sufficient
253 to induce tumors on its own (17). The MMTV-NIC transgene expresses both the ERBB2/NEU
254 oncoprotein and Cre from the MMTV promoter, assuring Cre expression, and thereby USP22
255 overexpression, in the same mammary epithelial cells at the same time as ERBB2/NEU
256 overexpression.

257

258 We monitored mammary tumor formation in MMTV-NIC mice bearing only the endogenous allele
259 of *Usp22* ($Usp22^{+/+}$) or bearing one ($Usp22^{OE/+}$) or two ($Usp22^{OE/OE}$) copies of the *Usp22 OE*
260 transgene in addition to the endogenous allele (**Fig. 1B**). As expected (22,26), the MMTV-NIC
261 mice all developed mammary epithelial tumors between ~120-150 days (T_{50}, median latency
262 period of 126 days). The kinetics and frequency of tumor formation were not altered by Usp22
263 overexpression, in either the $Usp22^{OE/+}$; NIC or $Usp22^{OE/OE}$; NIC mice (**Fig. 1B**). No significant

264 changes were observed in tumor weight, tumor volume, or numbers of tumors per mouse upon
265 Usp22 overexpression (**Fig. 1C, D** and **E**).
266
267 Consistent with these results, no increase in ERBB2, phospho-ERBB2, or ERα protein levels
268 were observed in mammary epithelial cells isolated from USP22 overexpressing mice, relative to
269 cells isolated from MMTV-NIC mice (**Fig. 2A**). Interestingly, a trend for increased incidence of
270 lung metastases was observed in both *Usp22*$^{OE/+}$ - NIC or *Usp22*$^{OE/OE}$ - NIC mice (**Fig. 2B**), which
271 may be related to decreased expression of E-CADHERIN and increased level of SLUG in
272 *Usp22*$^{OE/OE}$ mice (**Fig. 2C**). Expression of other markers of the epithelial-mesenchymal transition,
273 however, were not significantly changed upon USP22 overexpression. Altogether, these results
274 indicate that increased expression of USP22 does not further enhance the tumorigenicity of the
275 activated ERBB2/NEU oncogene in MMTV-NIC mice.
276
277 ***Usp22* deletion impacts tumor formation in MMTV-NIC mice**
278
279 We next sought to determine whether *Usp22* is required for tumorigenesis in MMTV-NIC mice
280 using the *Usp22*^{flox} (*Usp22*^{FL}) allele, which allows tissue specific deletion of *Usp22* upon exposure
281 to Cre (**Fig. 3A**). Loss of one allele of *Usp22* (*Usp22*$^{FL/+}$) had no impact on the kinetics of tumor
282 formation in MMTV-NIC mice (**Fig. 3B**). However, complete deletion of *Usp22* significantly
283 delayed tumor formation (T_{50} 214 days) with some mice remaining tumor free for almost 300 days
284 (**Fig. 3B**). Loss of *Usp22* impacted both weight and volume of tumors and substantially reduced
285 the numbers of tumors formed per mouse (**Fig. 3C, D** and **E**). These data are consistent with
286 those of Prokakis et al (21), who also observed reduced tumor burden upon loss of *Usp22* using
287 a different MMTV-Neu mouse model.
288
289 **Decreased expression of ERBB2 in MMTV-NIC mice**
290
291 To determine the molecular mechanisms underlying decreased tumor formation, we isolated
292 mammary epithelial cells (MECs) from MMTV-NIC mice with or without the *Usp22*^{FL} allele at an
293 early time point (100 days), before any tumors were observed in the MMTV-NIC mice.
294 Immunoblots confirmed partial and complete loss of USP22 protein in the *Usp22*$^{FL/+}$-NIC and
295 *Usp22*$^{FL/FL}$-NIC MECs, respectively. Remarkably, levels of GCN5 and ATXN7L3 were also
296 reduced in *Usp22*$^{FL/FL}$- NIC MECs, indicating potential loss of both the histone acetyltransferase
297 and the deubiquitinase modules in the SAGA complex upon *Usp22* deletion.

298

299 Loss of USP22 protein expression correlated with loss of *Usp22* mRNA in *Usp22*$^{FL/FL}$-NIC MECs
300 (**Fig. 4B**). Surprisingly, exogenous *Erbb2* RNA, protein, and phosphorylation levels were also
301 dramatically reduced upon loss of *Usp22* (**Fig. 4C** and **D**). Expression of endogenous mouse
302 ERBB3 was also decreased in *Usp22*$^{FL/FL}$- NIC MECs, consistent with cross regulation of ERBB2
303 and ERBB3 stability reported by others (22). No changes were observed in expression of heat
304 shock protein family members, HSP70, HSP90, or HSP90ab1 either in MECs or in end-stage
305 tumors isolated from *Usp22*$^{FL/FL}$ - NIC mice (**Fig. 4D** and **E**). These findings are in contrast to
306 those of Prokakis et al, who found no changes in ERBB2/HER2 expression by
307 immunohistochemistry of ERBB2/NEU induced tumors from *Usp22*$^{FL/FL}$ mice(21). This
308 discrepancy may reflect the different time points examined, as our analyses focused on events
309 before tumor formation rather than on the later tumor stages that did form in these mice.
310

311 The decreased expression of ERBB2/NEU observed in our *Usp22*$^{FL/FL}$-NIC mice is highly
312 consistent with the decreased tumor burden of these mice. However, these data reveal that the
313 impact of *Usp22* loss on tumorigenesis in this model system, and likely other MMTV driven NEU
314 mouse models, is due to changes in the activity of the MMTV promoter that drives expression of
315 the *Erbb2/Neu* transgene RNA (**Fig. 4C**).
316

317 ***Usp22* depletion does not affect ERBB2/HER2 expression in human cells**
318

319 To assess whether *USP22* loss might also impact ERBB2 protein levels independently of *ERBB2*
320 gene transcription changes, we depleted *USP22* in human MCF-10A cells that overexpress
321 *ERBB2*. Two independent shRNAs targeting *USP22* significantly depleted both USP22 RNA and
322 protein, with no effects on ERBB2 RNA or protein expression (**Figure 5A, B** and **C**). We further
323 confirmed these results using CRISPR/Cas9 targeting of *USP22*, and again saw no impact on
324 ERBB2 expression upon deletion of *USP22* in the MCF-10A-ERBB2 OE cells (**Fig. 5D**). Finally,
325 we examined ERBB2 levels with and without *USP22* depletion in two HER2-positive human
326 breast cancer cell lines, SKBR3 and HCC1954, and again saw no impact on ERBB2 protein levels
327 upon *USP22* loss (**Fig. 5E**). These results indicate that *USP22* does not impact ERBB2
328 expression driven by non-MMTV exogenous promoters or by the endogenous *ERBB2* promoter.
329 However, our results do not rule out effects on downstream factors in the ERBB2 signaling
330 cascade that impact tumorigenesis (27).
331

332

333 ***Usp22* loss of function impacts multiple factors required for MMTV promoter activity**

334

335 MMTV promoter activity is regulated by nuclear hormone receptors including glucocorticoid
336 receptor (GR), progesterone receptor (PR), androgen receptor, as well as by ATP-dependent
337 chromatin remodeling factors (28). The receptors bind to hormone response elements located in
338 the MMTV promoter and then recruit the SWI/SNF BRG1 complex and other coactivators to
339 activate the promoter (29-33). We compared expression of GR, PR, and BRG1 in MECs isolated
340 from 100 day old *Usp22*$^{+/+}$- NIC and *Usp22*$^{FL/FL}$- NIC mice. Loss of Usp22 resulted in decreased
341 levels of *Nr3c*1 transcript and protein (GR), and decreased levels of *PGR* transcript *(*PR*)* (**Fig.
342 6A, B** and **C**). Although *Smarca4* transcript (Brg1) was increased in the absence of *Usp22*,
343 protein levels were decreased (**Fig. 6C and D**), suggesting USP22 regulates BRG1 at a post-
344 transcriptional level, directly or indirectly. Diminished levels of GR, PR and BRG1 are consistent
345 with decreased MMTV promoter activity and decreased levels of Erbb2 observed in *Usp22*$^{FL/FL}$ -
346 NIC mic*e.*

347

348

349 **Discussion**

350

351 The role of USP22 overexpression in tumorigenesis and metastasis is an important question, as
352 it is associated with highly aggressive, therapy resistant cancers. Our mouse models clearly
353 established that overexpression of USP22 on its own is not sufficient to induce tumors (17). Here,
354 we report that USP22 overexpression does not accelerate or amplify tumorigenesis in MMTV-NIC
355 mice. This lack of effect could indicate a different mode of action for USP22 in tumor formation
356 or progression, or it may reflect the already very high activity and expression of the rat NEU
357 oncogene in these mice. The trend towards increased metastasis to the lung in USP22 OE
358 MMTV-NIC mice may indicate that facilitates downstream steps in cancer progression, such as
359 the epithelial-mesenchymal transition. Additional studies using a more attenuated oncogene are
360 needed to determine if USP22 augments both tumorigenesis or metastasis.

361

362 Our finding that loss of *Usp22* drastically hampers tumor formation in MMTV-NIC mice is
363 consistent with the results of Prokaris et al, who used a similar mouse model wherein ERBB2
364 expression and Cre were driven by the MMTV promoter, but in separate transgenes. Our data
365 clearly indicate that loss of *Usp22* strongly impacts *Erbb2/Neu* RNA and protein expression in

366 MECs isolated from 100-day old MMTV-NIC mice, before the time of the earliest tumor formation,
367 reflecting decreased activity of the MMTV promoter. Loss of exogenous EBB22/NEU expression
368 also impacted endogenous ERBB3 expression, further reducing tumorigenesis. Reduced levels
369 of ERBB2/NEU protein were also observed in end stage tumors from our MMTV-NIC *Usp22* null
370 mice, although more variability in expression was evident between mice and between tumors. In
371 contrast, Prokaris et al (21) reported no change in ERBB2 levels in their mice, although they only
372 presented measurements of levels of the oncogene in tumors by histology and did not examine
373 pre-tumor cells or tissues. These authors also reported down regulation of HSPA5, an HSP70
374 family member involved in the unfolded protein response, in tumors from *Usp22* null mice,
375 consistent with reports that USP22 mediates deubiquitination of HSPA5 in human prostate cancer
376 cells (15). Knock down of *USP22* in HCC1954 cells led to loss of HSPA5, indicating USP22 may
377 stabilize HSPA5 to suppress the unfolded protein response. Whether *Usp22* loss in pretumor
378 cells might impact tumor formation through changes in the UPR is not yet clear. Other studies by
379 this group indicated USP22 impacts stability of HSP90AB1 in prostate cancer and breast cancer
380 cells, including HCC1954 cells (34). We saw no effects on HSP90AB1, HSP90, or HSP70 protein
381 levels in our *Usp22* null MMTV-NIC mice at 100 days or on HSP90AB1 levels in end stage tumors
382 from these mice.
383
384 The impact on ERBB2/NEU expression levels that we observe is limited to the MMTV-NIC
385 transgene. Loss of *USP22* had no effect on *ERBB2* RNA or protein expression driven by the
386 CMV promoter in MCF10A cells or on endogenous ERBB2 protein expression in two HER2-
387 positive breast cancer cell lines, SKBR3 and HCC1954. However, these findings do not preclude
388 an impact of *Usp22* loss on downstream components of Erbb2 signaling. Indeed, deletion of
389 *Usp22* in mice or *in vitro*, in induced endothelial cells, led to decreased expression of several
390 common intermediates to receptor tyrosine kinase signaling, including Gab1 and Gab2, and
391 decreased phosphorylation of AKT and ERK1/2 (16). Additional studies using different, non-
392 MMTV transgene mouse models are needed to determine the impact of *Usp22* loss on these
393 factors in mammary tumors and to define the mechanisms underlying such effects.
394
395 Multiple preclinical studies in HER2-positive cells have been performed to understand the
396 molecular mechanism of therapy resistance, but the use of cancer cell lines as the primary model
397 system in those studies does not recapitulate the complexity and heterogeneity of tumorigenesis
398 in organisms. The limitations of conventional cell culture and mouse xenograft studies are well-
399 recognized as an obstacle to the effective translation of preclinical findings into therapy (35).

Mouse models for HER2-driven mammary tumorigenesis have been used extensively and the MMTV-NIC mouse is among the most commonly analyzed (36). Our work draws attention to caveats in the interpretations of Erbb2 regulation when it is under the control of exogenous promoters like MMTV. Loss of *Usp22* impacts MMTV promoter activity, likely through down regulation of BRG1, PR and GR. These factors themselves impact cancer formation and progression. PR is a well-established breast cancer biomarker in evaluating prognosis and response to treatment. GR plays key roles in breast cancer metastasis and response to treatment (37). TCGA analysis reveals high frequency of BRG1 overexpression, but low frequency of BRG1 mutation, in invasive breast cancer (38,39). Given the importance of each of these factors in gene regulation and cancer, further delineation of USP22 functions in regulation of BRG1, PR, and GR could provide new insights to its roles in cancer formation and progression. The recent report of novel USP22 specific inhibitors (40) provides strong impetus for fully understanding the functions of this DUB in both normal cells and in cancers.

Conflicts of Interest

The authors have no competing financial interests to disclose.

Acknowledgments

We would like to thank Pam Whitney at the Flow Cytometry and Cell Imaging Core Facility-Department of Epigenetics and Molecular Carcinogenesis (EMC), MD Anderson Cancer Center and CPRIT Core Facility Support Grant (RP170628) for the support on GFP+ cell sorting experiments. We thank Debra Hollowell for assistance with mouse *in vitro* fertilization. We thank Dr. Lezlee Coghlan, Amanda Martin and animal facility staff for their help in determining tumor size and animal husbandry. We also thank Dr. Dihua Yu (MD Anderson Cancer Center) for providing us MCF10A-vec and MCF10A-*ERBB2* OE cell lines, and Dr. László Tora for providing the anti-ATXN7L3 antibody. We would also like to thank all members of the Dent lab for their advice in experimental procedures. This work was largely supported by the National Institutes of Health grant R01HD094400 to S.Y.R. Dent. This study made use of the Research Animal Support Facility-Smithville (including Laboratory Animal Genetic Services), supported by P30 CA016672 DHHS/NCI Cancer Center Support Grant to MD Anderson Cancer Center.

Authors' Contributions

Conception and design: X. Kuang, S.Y.R. Dent and E. Koutelou.

Methodology: X. Kuang, F. Benavides, W.J. Muller, S.Y.R. Dent and E. Koutelou.

Data curation: X. Kuang and E. Koutelou.

Formal analysis: X. Kuang., S.Y.R. Dent. and E. Koutelou.

Investigation: X. Kuang.

Validation: X. Kuang., A. Salinger.

Project administration: X. Kuang, S.Y.R. Dent. and E. Koutelou.

Supervision: S.Y.R. Dent and E. Koutelou.

Funding acquisition: S.Y.R. Dent.

Writing—original draft: X. Kuang, S.Y.R. Dent and E. Koutelou.

Writing, review, and/or revision of the manuscript: X. Kuang, S.Y.R. Dent and E. Koutelou. All authors have read and agreed to this submitted version of the manuscript.

479 **Figure legends**

480

481 **Figure 1**.

482 Overexpression of USP22 does not augment mammary gland tumor formation in MMTV-NIC
483 mice. **A**. Schematic representation of *Rosa26KI-Usp22-LSL* mice that were crossed with MMTV-
484 NIC mice to generate USP22-OE-MMTV-NIC progeny. **B**. Kaplan-Meier curve showing tumor-
485 free survival, comparing *Usp22*$^{+/+}$- NIC (n=41), *Usp22*$^{OE/+}$- NIC (n=37) and *Usp22*$^{OE/OE}$- NIC (n=39)
486 mice. p=0.012 was determined by Log-rank (Mantel–Cox) test, comparing *Usp22*$^{OE/OE}$- NIC mice
487 with *Usp22*$^{+/+}$-NIC mice. **C-E**. Tumor weight (**C),** tumor volume (**D**) and **n**umber of tumors per
488 animal (**E)** were measured in *Usp22*$^{+/+}$-NIC (n=7), *Usp22*$^{OE/+}$-NIC (n=5) and *Usp22*$^{OE/OE}$-NIC mice
489 (n=6). Tumors were harvested 45-55 days after tumor was first palpable (tumor onset). ns: No
490 statistical significance when compared *Usp22*$^{OE/OE}$*-NIC* mice with *Usp22*$^{+/+}$*-NIC* mice using two-
491 tailed unpaired t test.

492

493 **Figure 2.**

494 Expression levels of ERBB2 and ERα proteins and incidence of lung metastases in *Usp22* $^{OE/OE}$-
495 NIC mice. **A.** Immunoblot analyses using lysates from endpoint tumors (n=3 for each group)
496 showed no difference in the levels of ERBB2 and ERα protein levels upon overexpression of
497 USP22 in *Usp22*$^{OE/OE}$- NIC mice. Levels of phosphorylated ERBB2 protein are also unaffected by
498 USP22 overexpression. **B.** Incidence of lung metastasis observed in *Usp22*$^{+/+}$-NIC (n=19),
499 *Usp22*$^{OE/+}$-NIC (n=22) and *Usp22*$^{OE/OE}$- NIC (n=22) mice. **C**. Immunoblot analysis using lysates
500 from endpoint tumors (n=3 for each group) showed decreased protein levels of E-CADHERIN and
501 increased levels of SLUG protein in *Usp22* $^{OE/OE}$ NIC/+ mice when compared with *Usp22* $^{+/+}$- NIC
502 mice. EMT markers like OCCLUDIN, VIMENTIN and TWIST were not significantly affected by
503 USP22 overexpression.

504

505 **Figure 3.**

506 Delayed tumor formation upon conditional deletion of *Usp22* in mammary gland epithelial cells in
507 MMTV-NIC mice. **A.** Schematic representation *Usp22* floxed mice crossed with MMTV-NIC mice
508 to generate of *Usp22*$^{FL/FL}$*-NIC* progeny. **B.** Kaplan-Meier curve showing tumor-free survival of
509 animals, comparing *Usp22*$^{+/+}$- NIC (n=20), *Usp22*$^{FL/+}$- NIC (n=18) and *Usp22*$^{FL/FL}$- NIC (n=21)
510 mice. p<0.0001 was determined by Log-rank (Mantel–Cox) test. **C-E**. Tumor weight (**C**), **t**umor
511 volume (**D)** and number of tumors per animal (**E)** measured in *Usp22*$^{+/+}$- NIC (n=11; p=0.0015),
512 *Usp22*$^{FL/+}$- NIC (n=5; p=0.0027) and *Usp22*$^{FL/FL}$- NIC mice (n=14; p<0.0001). P values were

513 determined by two-tailed unpaired t test when compared *Usp22*$^{FL/FL}$ -NIC mice with *Usp22*$^{+/+}$-NIC
514 mice.
515
516 **Figure 4.**
517 Decreased expression of SAGA components, ERBB2, and ERBB3 upon deletion of *Usp22* in
518 mammary gland epithelial cells (MECs) collected from 100-day old NIC mice. **A.** Immunoblot
519 analyses showed decreased levels of USP22, GCN5 and ATXN7L3 proteins in MECs collected
520 from *Usp22*$^{FL/FL}$*-NIC* mice compared to *Usp22*$^{+/+}$ *-NIC* and *Usp22*$^{FL/+}$ *-NIC* mice. n=3 for each
521 group. **B, C.** qRT-PCR analysis of total RNA collected from *Usp22*$^{FL/FL}$*- NIC* MECs confirmed that
522 mRNA levels of *Usp22* and *Erbb2* were drastically decreased compared to *Usp22*$^{+/+}$*- NIC*.
523 $p<0.0001$ for both *Usp22* and *Erbb2*, as determined by two-tailed unpaired t test. n=5 for each
524 group. Each sample was measured in triplicates **D.** Immunoblot analyses showed decreased
525 levels of ERBB2 and ERBB3 proteins in MECs collected from *Usp22*$^{FL/FL}$*- NIC* mice compared to
526 *Usp22*$^{+/+}$*- NIC* and *Usp22*$^{FL/+}$- NIC mice. HSP70, HSP90AB1 and HSP90 protein levels were not
527 affected when analyzed by western blotting in the same lysates. n=3 for each group. **E.**
528 Immunoblot analyses using lysates from endpoint tumors from *Usp22*$^{FL/FL}$*- NIC* mice showed that
529 levels of USP22, ERBB2, ERBB3, phospho-ERK and H2Bub decreased relative to other
530 genotypes, but levels of HSP90AB1 and GCN5 did not change. n=3 for each group.
531
532 **Figure 5.**
533 Depletion or deletion of *USP22* in MCF10A cells that stably overexpress ERBB2 did not affect the
534 levels of ERBB2. **A.** Efficient depletion of *USP22* by lentiviral shRNA knock down in MCF10A-
535 ERBB2 cells as verified by qRT-PCR analysis. **B.** qRT-PCR analysis indicate levels of *ERBB2*
536 mRNA did not change upon *USP22* shRNA knock down. ns: No statistical significance. **C.**
537 Immunoblot analysis of MCF10A-ERBB2 cell lysates showed that ERBB2 protein levels are not
538 changed upon *USP22* shRNA knock down. **D.** Immunoblot analysis of MCF10A-ERBB2 cell
539 lysates indicate that ERBB2 protein levels are not changed upon *USP22* CRISPR/Cas9 knockout.
540 **E.** Immunoblot analysis of HER2-positive SKBR3 and HCC1954 cell lysates showed no difference
541 in ERBB2 protein levels upon *USP22* shRNA knock down**.**
542
543 **Figure 6.**
544 Expression levels of *Nr3c1* (glucocorticoid receptor), *Pgr* (progesterone receptor) and *Smarca4*
545 *(*BRG1*)* upon loss of *Usp22*. **A, B, C.** qRT-PCR analysis of total RNA collected from *Usp22*$^{FL/FL}$*-*
546 *NIC* MECs revealed decreased levels of *Nr3c1* and *Pgr,* but increased levels of *Smarca4 (Brg1)*

547 compared to *Usp22* $^{+/+}$- *NIC* mice. p=0.0026 for *Nr3c1*, p=0.0053 for *PGR* and p=0.0012 for
548 *Smarca4* were determined by two-tailed unpaired t test. n=3-4 for each group. **D.** Immunoblot
549 analyses indicate decreased levels of GR and BRG1 proteins in MECs collected from *Usp22*$^{FL/FL}$-
550 NIC mice compared to *Usp22* $^{+/+}$- NIC and *Usp22* $^{FL/+}$- NIC mice. n=3 for each group.
551
552
553
554
555
556
557
558
559
560
561
562
563
564
565
566
567
568
569
570
571
572
573
574
575
576
577
578
579
580

581 **References**

582
583

584 1. Wang L, Dent SY. Functions of SAGA in development and disease. Epigenomics
585 **2014**;6:329-39
586 2. Glinsky GV. Death-from-cancer signatures and stem cell contribution to metastatic
587 cancer. Cell Cycle **2005**;4:1171-5
588 3. Glinsky GV, Berezovska O, Glinskii AB. Microarray analysis identifies a death-from-
589 cancer signature predicting therapy failure in patients with multiple types of cancer. J
590 Clin Invest **2005**;115:1503-21
591 4. Farria AT, Mustachio LM, Akdemir ZHC, Dent SYR. GCN5 HAT inhibition reduces
592 human Burkitt lymphoma cell survival through reduction of MYC target gene expression
593 and impeding BCR signaling pathways. Oncotarget **2019**;10:5847-58
594 5. Farria AT, Plummer JB, Salinger AP, Shen J, Lin K, Lu Y*, et al.* Transcriptional
595 Activation of MYC-Induced Genes by GCN5 Promotes B-cell Lymphomagenesis.
596 Cancer Res **2020**;80:5543-53
597 6. Wang L, Koutelou E, Hirsch C, McCarthy R, Schibler A, Lin K*, et al.* GCN5 Regulates
598 FGF Signaling and Activates Selective MYC Target Genes during Early Embryoid Body
599 Differentiation. Stem Cell Reports **2018**;10:287-99
600 7. Mustachio LM, Roszik J, Farria AT, Guerra K, Dent SY. Repression of GCN5 expression
601 or activity attenuates c-MYC expression in non-small cell lung cancer. Am J Cancer Res
602 **2019**;9:1830-45
603 8. Liu YL, Jiang SX, Yang YM, Xu H, Liu JL, Wang XS. USP22 acts as an oncogene by
604 the activation of BMI-1-mediated INK4a/ARF pathway and Akt pathway. Cell Biochem
605 Biophys **2012**;62:229-35
606 9. Lin Z, Yang H, Kong Q, Li J, Lee SM, Gao B*, et al.* USP22 antagonizes p53
607 transcriptional activation by deubiquitinating Sirt1 to suppress cell apoptosis and is
608 required for mouse embryonic development. Mol Cell **2012**;46:484-94
609 10. Gennaro VJ, Stanek TJ, Peck AR, Sun Y, Wang F, Qie S*, et al.* Control of CCND1
610 ubiquitylation by the catalytic SAGA subunit USP22 is essential for cell cycle
611 progression through G1 in cancer cells. Proc Natl Acad Sci U S A **2018**;115:E9298-e307
612 11. Zhou A, Lin K, Zhang S, Chen Y, Zhang N, Xue J*, et al.* Nuclear GSK3β promotes
613 tumorigenesis by phosphorylating KDM1A and inducing its deubiquitylation by USP22.
614 Nature cell biology **2016**;18:954-66
615 12. Schrecengost RS, Dean JL, Goodwin JF, Schiewer MJ, Urban MW, Stanek TJ*, et al.*
616 USP22 regulates oncogenic signaling pathways to drive lethal cancer progression. Cancer
617 Res **2014**;74:272-86
618 13. Kosinsky RL, Zerche M, Saul D, Wang X, Wohn L, Wegwitz F*, et al.* USP22 exerts
619 tumor-suppressive functions in colorectal cancer by decreasing mTOR activity. Cell
620 Death Differ **2020**;27:1328-40
621 14. Atanassov BS, Evrard YA, Multani AS, Zhang Z, Tora L, Devys D*, et al.* Gcn5 and
622 SAGA regulate shelterin protein turnover and telomere maintenance. Mol Cell
623 **2009**;35:352-64
624 15. McCann JJ, Vasilevskaya IA, Poudel Neupane N, Shafi AA, McNair C, Dylgjeri E*, et al.*
625 USP22 Functions as an Oncogenic Driver in Prostate Cancer by Regulating Cell
626 Proliferation and DNA Repair. Cancer Res **2020**;80:430-43

627 16. Koutelou E, Wang L, Schibler AC, Chao HP, Kuang X, Lin K*, et al.* USP22 controls
628 multiple signaling pathways that are essential for vasculature formation in the mouse
629 placenta. Development **2019**;146
630 17. Kuang X, McAndrew MJ, Mustachio LM, Chen YC, Atanassov BS, Lin K*, et al.* Usp22
631 Overexpression Leads to Aberrant Signal Transduction of Cancer-Related Pathways but
632 Is Not Sufficient to Drive Tumor Formation in Mice. Cancers (Basel) **2021**;13
633 18. Muller WJ, Sinn E, Pattengale PK, Wallace R, Leder P. Single-step induction of
634 mammary adenocarcinoma in transgenic mice bearing the activated c-neu oncogene. Cell
635 **1988**;54:105-15
636 19. Moody SE, Sarkisian CJ, Hahn KT, Gunther EJ, Pickup S, Dugan KD*, et al.* Conditional
637 activation of Neu in the mammary epithelium of transgenic mice results in reversible
638 pulmonary metastasis. Cancer Cell **2002**;2:451-61
639 20. Ursini-Siegel J, Schade B, Cardiff RD, Muller WJ. Insights from transgenic mouse
640 models of ERBB2-induced breast cancer. Nat Rev Cancer **2007**;7:389-97
641 21. Prokakis E, Dyas A, Grün R, Fritzsche S, Bedi U, Kazerouni ZB*, et al.* USP22 promotes
642 HER2-driven mammary carcinoma aggressiveness by suppressing the unfolded protein
643 response. Oncogene **2021**;40:4004-18
644 22. Siegel PM, Ryan ED, Cardiff RD, Muller WJ. Elevated expression of activated forms of
645 Neu/ErbB-2 and ErbB-3 are involved in the induction of mammary tumors in transgenic
646 mice: implications for human breast cancer. Embo j **1999**;18:2149-64
647 23. Farley FW, Soriano P, Steffen LS, Dymecki SM. Widespread recombinase expression
648 using FLPeR (flipper) mice. Genesis **2000**;28:106-10
649 24. Bray K, Gillette M, Young J, Loughran E, Hwang M, Sears JC*, et al.* Cdc42
650 overexpression induces hyperbranching in the developing mammary gland by enhancing
651 cell migration. Breast Cancer Res **2013**;15:R91
652 25. Lu J, Guo H, Treekitkarnmongkol W, Li P, Zhang J, Shi B*, et al.* 14-3-3zeta Cooperates
653 with ErbB2 to promote ductal carcinoma in situ progression to invasive breast cancer by
654 inducing epithelial-mesenchymal transition. Cancer Cell **2009**;16:195-207
655 26. Ursini-Siegel J, Hardy WR, Zuo D, Lam SH, Sanguin-Gendreau V, Cardiff RD*, et al.*
656 ShcA signalling is essential for tumour progression in mouse models of human breast
657 cancer. Embo j **2008**;27:910-20
658 27. Feng Y, Spezia M, Huang S, Yuan C, Zeng Z, Zhang L*, et al.* Breast cancer development
659 and progression: Risk factors, cancer stem cells, signaling pathways, genomics, and
660 molecular pathogenesis. Genes Dis **2018**;5:77-106
661 28. Kinyamu HK, Archer TK. Modifying chromatin to permit steroid hormone receptor-
662 dependent transcription. Biochim Biophys Acta **2004**;1677:30-45
663 29. Chen J, Kinyamu HK, Archer TK. Changes in attitude, changes in latitude: nuclear
664 receptors remodeling chromatin to regulate transcription. Mol Endocrinol **2006**;20:1-13
665 30. Fryer CJ, Archer TK. Chromatin remodelling by the glucocorticoid receptor requires the
666 BRG1 complex. Nature **1998**;393:88-91
667 31. Huang ZQ, Li J, Sachs LM, Cole PA, Wong J. A role for cofactor-cofactor and cofactor-
668 histone interactions in targeting p300, SWI/SNF and Mediator for transcription. Embo j
669 **2003**;22:2146-55
670 32. Johnson TA, Elbi C, Parekh BS, Hager GL, John S. Chromatin remodeling complexes
671 interact dynamically with a glucocorticoid receptor-regulated promoter. Mol Biol Cell
672 **2008**;19:3308-22

673 33. Trotter KW, Archer TK. Reconstitution of glucocorticoid receptor-dependent
674 transcription in vivo. Mol Cell Biol **2004**;24:3347-58
675 34. Kosinsky RL, Helms M, Zerche M, Wohn L, Dyas A, Prokakis E*, et al.* USP22-
676 dependent HSP90AB1 expression promotes resistance to HSP90 inhibition in mammary
677 and colorectal cancer. Cell Death Dis **2019**;10:911
678 35. Sharpless NE, Depinho RA. The mighty mouse: genetically engineered mouse models in
679 cancer drug development. Nat Rev Drug Discov **2006**;5:741-54
680 36. Taneja P, Frazier DP, Kendig RD, Maglic D, Sugiyama T, Kai F*, et al.* MMTV mouse
681 models and the diagnostic values of MMTV-like sequences in human breast cancer.
682 Expert Rev Mol Diagn **2009**;9:423-40
683 37. Dietrich N, Hoffman JA, Archer TK. BAF Complexes and the Glucocorticoid Receptor
684 in Breast Cancers. Curr Opin Endocr Metab Res **2020**;15:8-14
685 38. Bai J, Mei P, Zhang C, Chen F, Li C, Pan Z*, et al.* BRG1 is a prognostic marker and
686 potential therapeutic target in human breast cancer. PLoS One **2013**;8:e59772
687 39. Marquez SB, Thompson KW, Lu L, Reisman D. Beyond Mutations: Additional
688 Mechanisms and Implications of SWI/SNF Complex Inactivation. Front Oncol
689 **2014**;4:372
690 40. Morgan M, Ikenoue T, Suga H, Wolberger C. Potent macrocycle inhibitors of the human
691 SAGA deubiquitinating module. Cell Chem Biol **2022**;29:544-54.e4
692
693
694

Kuang et al. Figure 1

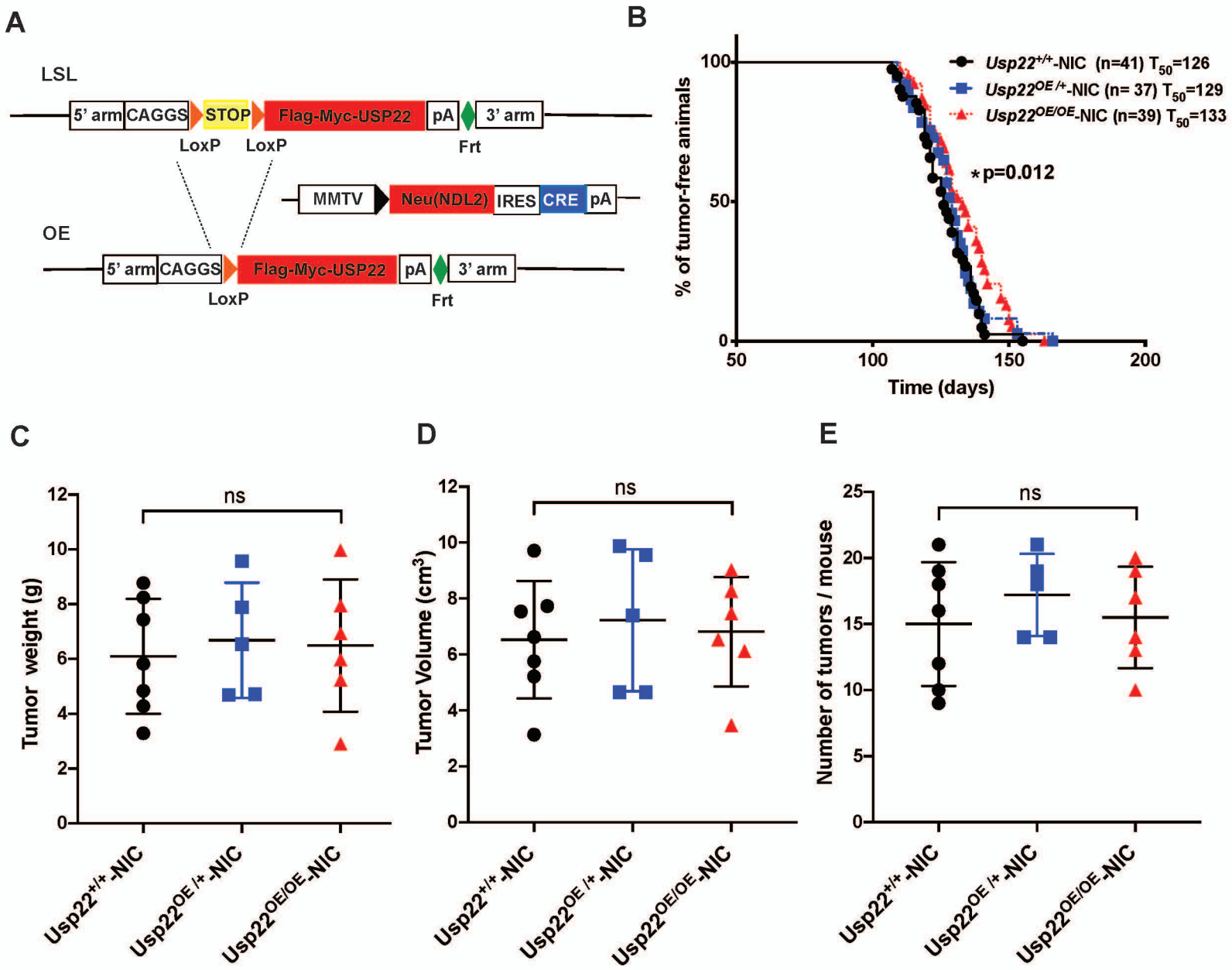

A

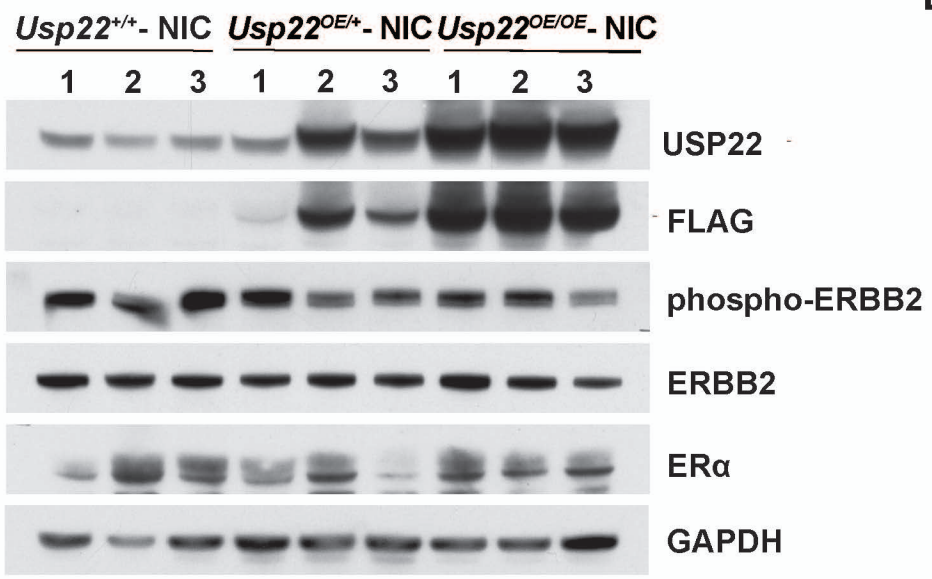
Usp22+/+- NIC
Usp22OE/+- NIC
Usp22OE/OE- NIC
1 2 3 1 2 3 1 2 3
USP22
FLAG
phospho-ERBB2
ERBB2
ERα
GAPDH

B

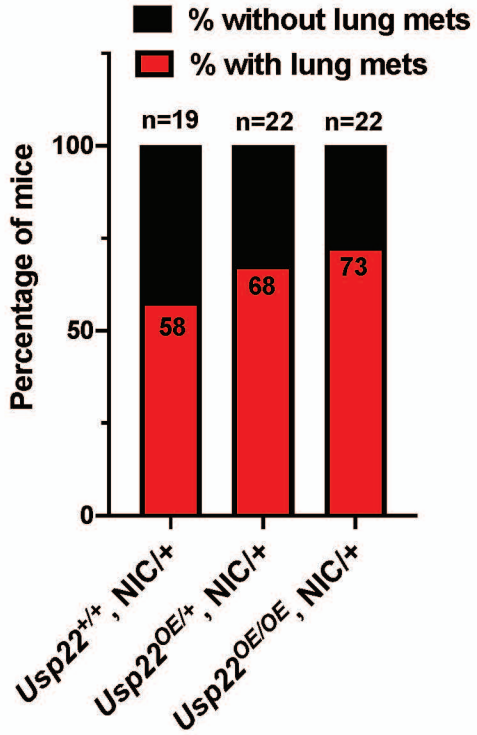
% without lung mets
% with lung mets
n=19
n=22
n=22
Percentage of mice
100
50
0
58
68
73
Usp22+/+ , NIC/+
Usp22OE/+ , NIC/+
Usp22OE/OE , NIC/+

C

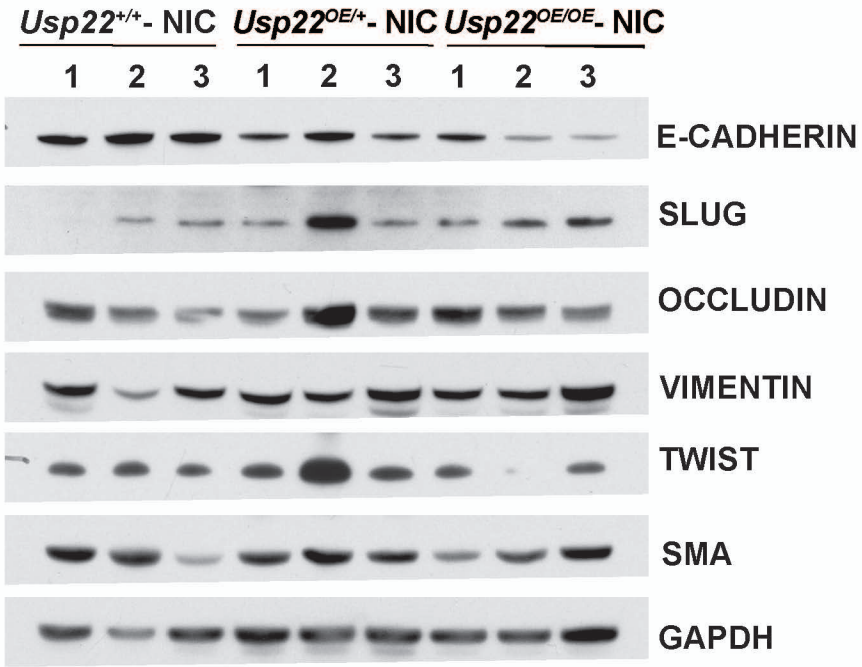
Usp22+/+- NIC
Usp22OE/+- NIC
Usp22OE/OE- NIC
1 2 3 1 2 3 1 2 3
E-CADHERIN
SLUG
OCCLUDIN
VIMENTIN
TWIST
SMA
GAPDH

Kuang et al. Figure 3

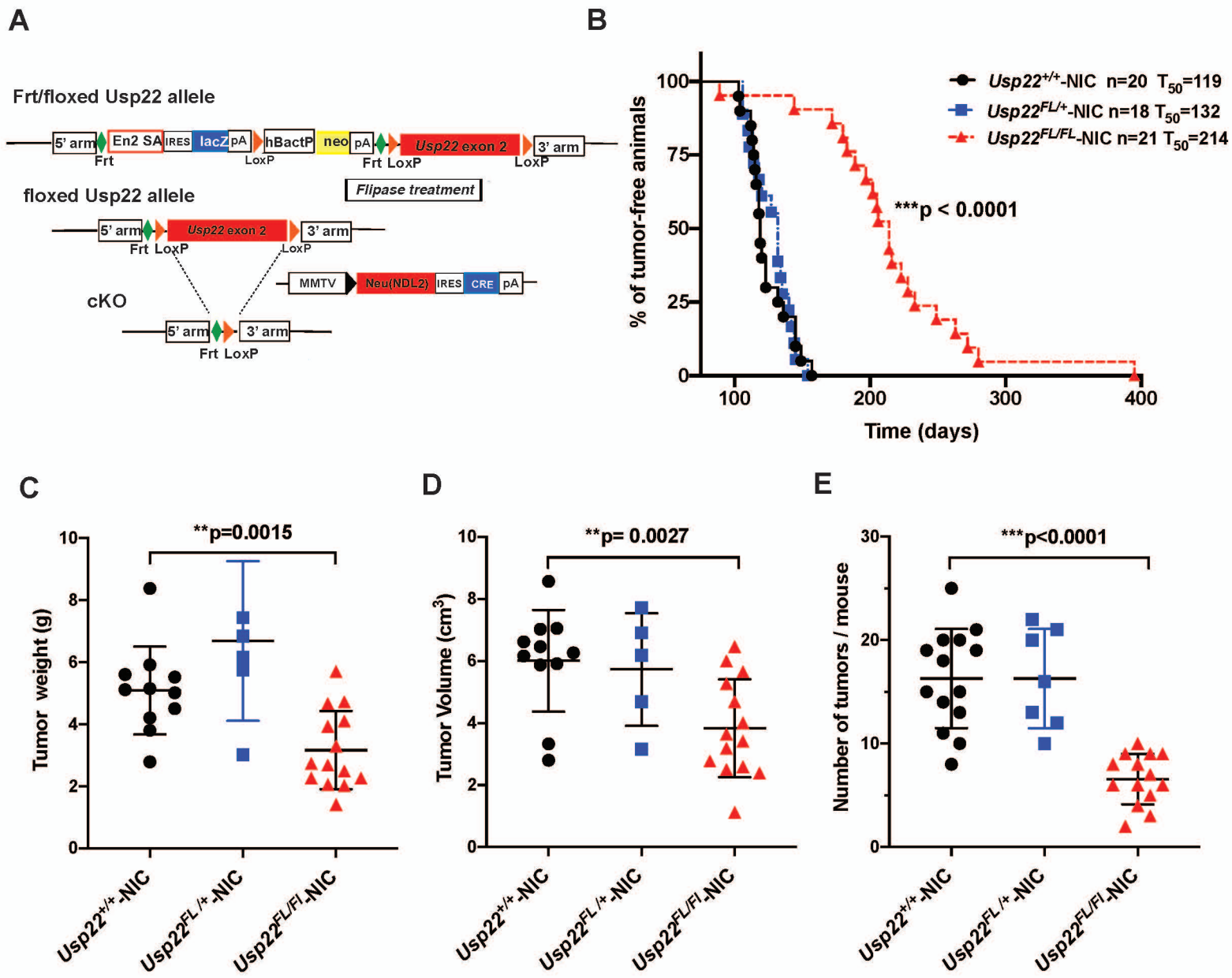

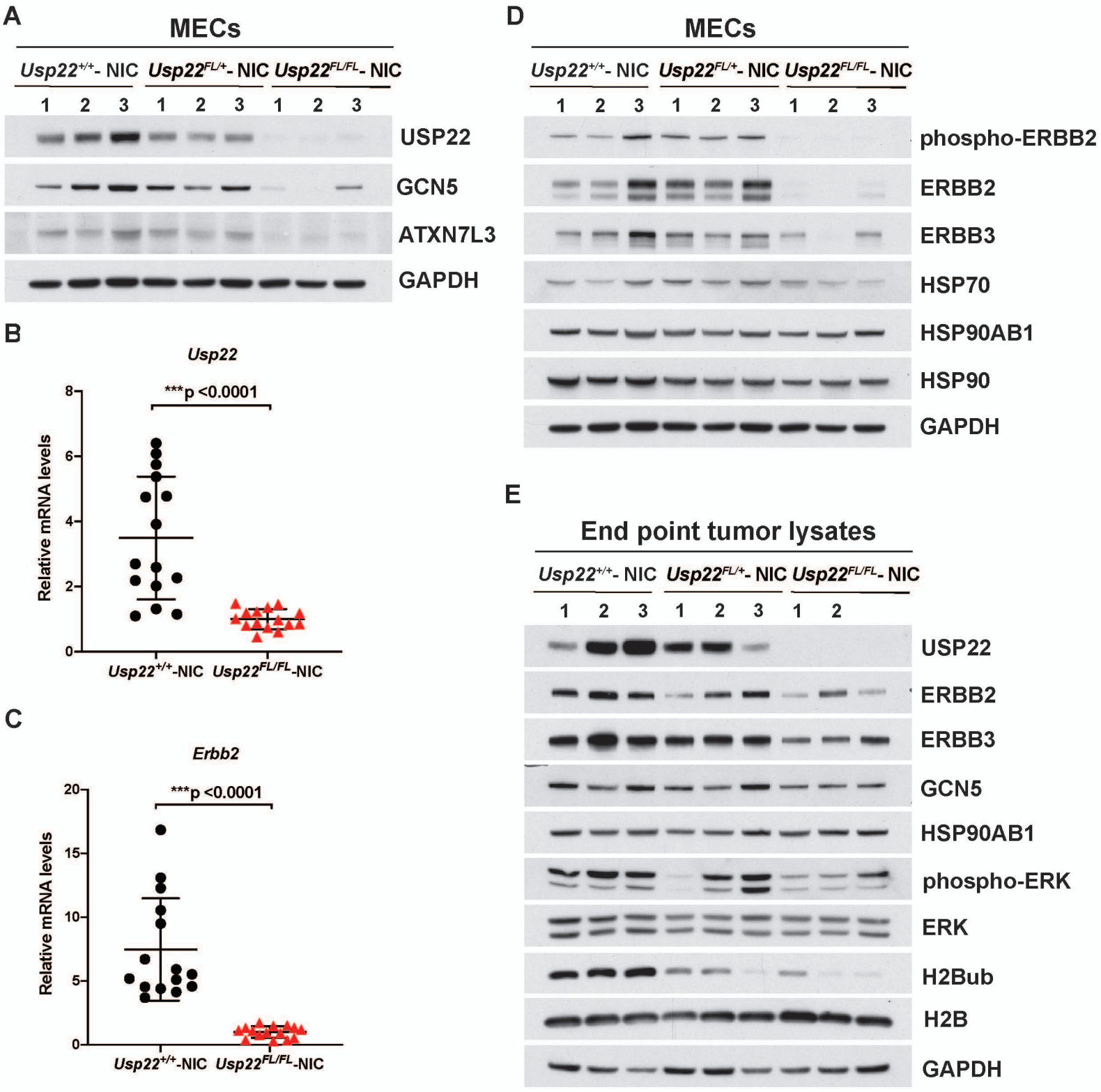
A
MECs
Usp22+/+- NIC
Usp22FL/+- NIC
Usp22FL/FL- NIC
1 2 3 1 2 3 1 2 3
USP22
GCN5
ATXN7L3
GAPDH
B
Usp22
***p <0.0001
Relative mRNA levels
0
2
4
6
8
Usp22+/+-NIC
Usp22FL/FL-NIC
C
Erbb2
***p <0.0001
Relative mRNA levels
0
5
10
15
20
Usp22+/+-NIC
Usp22FL/FL-NIC
D
MECs
Usp22+/+- NIC
Usp22FL/+- NIC
Usp22FL/FL- NIC
1 2 3 1 2 3 1 2 3
phospho-ERBB2
ERBB2
ERBB3
HSP70
HSP90AB1
HSP90
GAPDH
E
End point tumor lysates
Usp22+/+- NIC
Usp22FL/+- NIC
Usp22FL/FL- NIC
1 2 3 1 2 3 1 2
USP22
ERBB2
ERBB3
GCN5
HSP90AB1
phospho-ERK
ERK
H2Bub
H2B
GAPDH

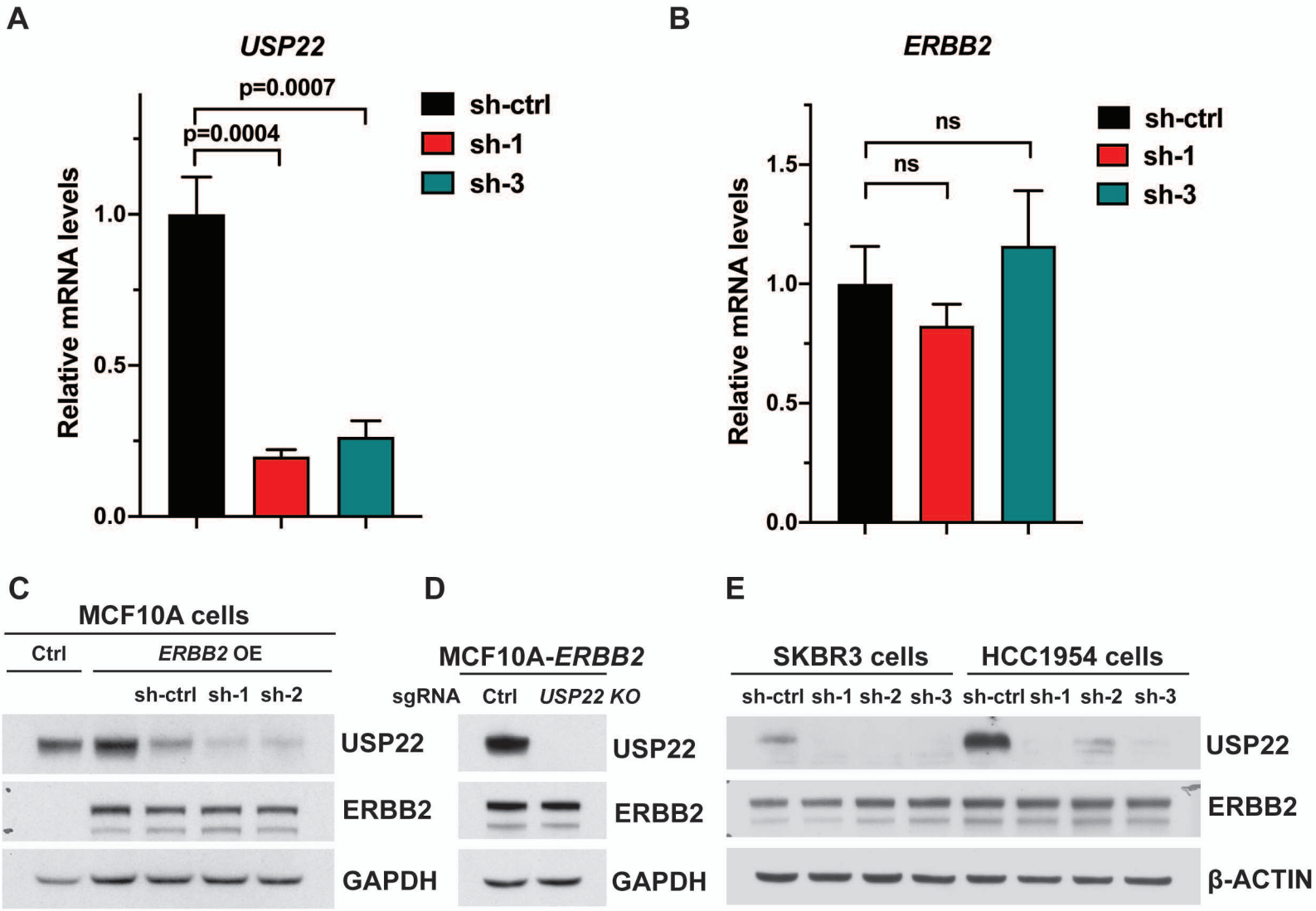
A
USP22
p=0.0007
p=0.0004
sh-ctrl
sh-1
sh-3
Relative mRNA levels
1.0
0.5
0.0
B
ERBB2
ns
ns
sh-ctrl
sh-1
sh-3
Relative mRNA levels
1.5
1.0
0.5
0.0
C
MCF10A cells
Ctrl
ERBB2 OE
sh-ctrl sh-1 sh-2
USP22
ERBB2
GAPDH
D
MCF10A-ERBB2
sgRNA Ctrl USP22 KO
USP22
ERBB2
GAPDH
E
SKBR3 cells
HCC1954 cells
sh-ctrl sh-1 sh-2 sh-3 sh-ctrl sh-1 sh-2 sh-3
USP22
ERBB2
β-ACTIN

A

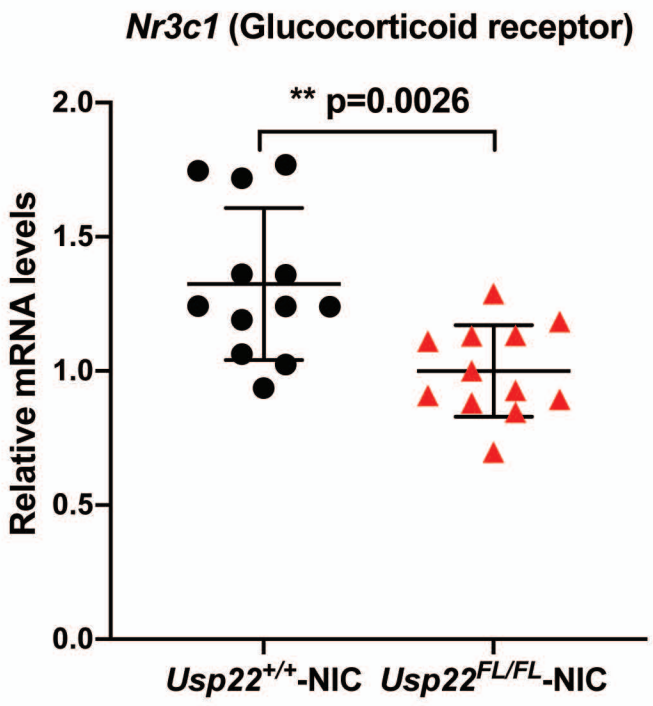
Nr3c1 (Glucocorticoid receptor)
** p=0.0026
Relative mRNA levels
2.0
1.5
1.0
0.5
0.0
Usp22+/+-NIC
Usp22FL/FL-NIC

B

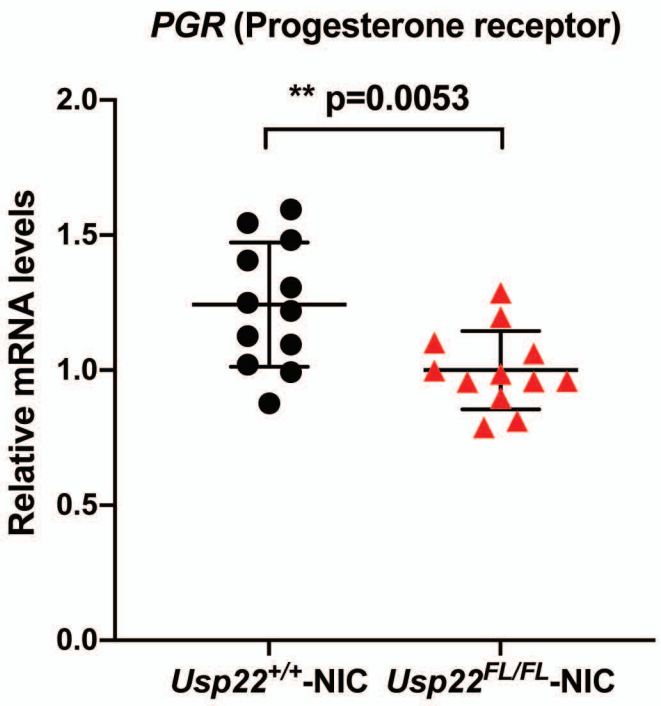
PGR (Progesterone receptor)
** p=0.0053
Relative mRNA levels
2.0
1.5
1.0
0.5
0.0
Usp22+/+-NIC
Usp22FL/FL-NIC

C

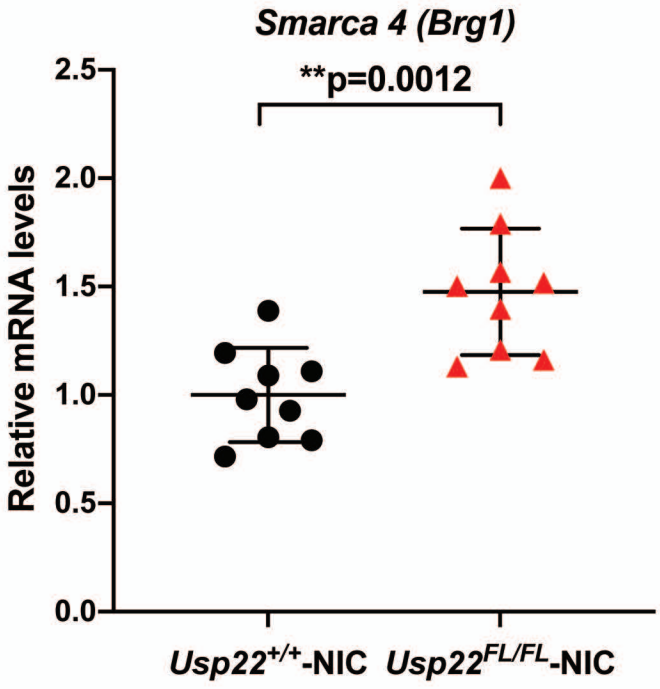
Smarca 4 (Brg1)
**p=0.0012
Relative mRNA levels
2.5
2.0
1.5
1.0
0.5
0.0
Usp22+/+-NIC
Usp22FL/FL-NIC

D

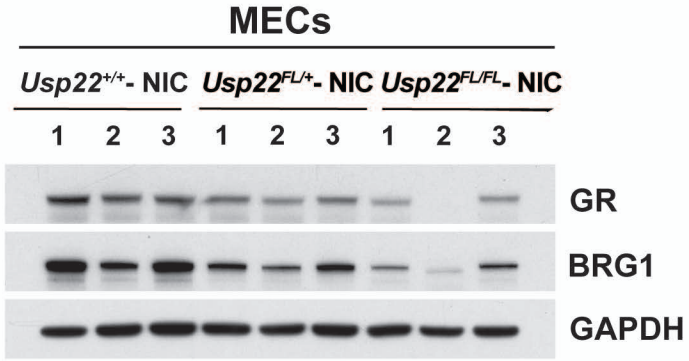
MECs
Usp22+/+- NIC
Usp22FL/+- NIC
Usp22FL/FL- NIC
1 2 3 1 2 3 1 2 3
GR
BRG1
GAPDH